CrossMark

Application of Central Composite Design for the Optimization of Reverse-Phase HPLC/DAD Separation of the *cis*- and *trans*-Isomers of Long-Chain Unsaturated Fatty Acids

Fatma Nur Arslan[1] · Hacer Azak[1]

Abstract The study deals with the optimization of reverse-phase HPLC separation of *cis*-/*trans*- isomers of long-chain unsaturated fatty acids by the assessment of the central composite design (CCD) of response surface methodology (RSM). The optimized conditions were also applied for the analysis of fatty acids in functional cold-pressed oils. The data obtained from experimental applications of CCD was used to model the parameters that significantly affect separations. The independent variables chosen were *flow rate* (X_1), *column temperature* (X_2), and *acetonitrile content in mobile phase* (X_3). A second-order polynomial model was used to estimate the impact of variables on separation efficiencies of the C30 and C18 stationary phases. The proposed CCD models were also validated with the ANOVA. The predicted values were in good agreement with experimental data, advising expert application of CCD as an option to obtain maximum information for the modeling of reverse-phase HPLC separation with little number of experiments. The optimal values of method parameters for the efficient C18 and C30 column separations as part of the k' response value were found to be flow rate of 1.10 and 0.42 mL min^{-1}, temperature of 3.6 and 9.4 °C, and acetonitrile content in mobile phase of 100 and 77.4%, respectively. ANOVA test results also illustrate that the CCD models can be successfully used to predict the optimum method parameters. To maximize both sensitivity and precision of the methods, the validation procedure was also performed and the higher correlation coefficients ($r = 0.9149$–0.9993) were determined for all fatty acid methyl esters. Thus, the proposed experimental designs were shown to offer considerable advantages over traditional method optimization approaches.

Keywords Unsaturated fatty acids · Central composite design · Optimization · Reverse-phase HPLC

✉ Fatma Nur Arslan
nurarslan@kmu.edu.tr

Hacer Azak
hacerazak1@gmail.com

[1] Department of Chemistry, Faculty of Science, University of Karamanoglu Mehmetbey, 70100 Karaman, Turkey

Introduction

Fatty acids (FAs) are the main components of most naturally occurring lipids in both animals and plants. Being part of almost all lipid molecules, FAs play crucial roles in living organisms (Lima and Abdalla 2002; Chen and Chuang 2002; Makahleh et al. 2010). The FA contained in natural samples are generally composed of a mixture of saturated and unsaturated FAs in *cis*- or *trans*- forms, with chain lengths varying from 4 to 28 carbon atoms. The variety of chain length, degree of unsaturation, geometry, and position of double bonds render their composition the most descriptive characteristic of these lipids and their origin (Ruiz-Rodriguez et al. 2010; Li et al. 2011). Hence, the analysis of FA profiles is of great importance in the control of industrial products, medical diagnostics, and testing of purity, origin, or shelf life studies (Makahleh et al. 2010; Bravi et al. 2006).

Due to the excellent separation power, chromatographic techniques are capable of quantitatively analyzing FAs for fats and oils, and have been in use for many decades. Most commonly used chromatographic techniques for the determination of FA compositions are gas chromatography (GC) and high-pressure liquid chromatography (HPLC) (Chen and Chuang

2002; Makahleh et al. 2010; Ruiz-Rodriguez et al. 2010; Li et al. 2011; Bravi et al. 2006; Bailey and Southon 1998). GC has been the method of choice for separation and quantification of FAs for a long time, usually after their derivatization. The use of modern GC systems coupled with a flame ionization (FID) or mass detector (MS) provides a high resolution for FA analysis (Rioux et al. 1999; Gutnikov 1995; Lacaze et al. 2007). However, GC methods have some inherent limitations for FA analysis. The first limitation is losing short-chain FAMEs when refluxing the esterification medium due to their volatile properties. The second significant limitation is problems result from potential thermal degradation and structural alteration of polyunsaturated FAs during their translation to methyl esters. The most important limitation is impeding the FAs' recovery for further analysis because the FID or MS detection destroys. The HPLC analysis of FAs, therefore, offers valuable opportunities to GC analysis for accurate quantitative analysis where authentication of peak characteristics is required (Chen and Chuang 2002; Gutnikov 1995; Molnár-Perl 2000).

A great advantage of HPLC methods over GC methods is that the eluted FAs are not destroyed during their detection. So, HPLC methods make possible the collection of desired fractions of FAs for further analysis (Lima and Abdalla 2002; Ruiz-Rodriguez et al. 2010; Wang et al. 2009; Wu et al. 2016). HPLC methods also enable the lower temperature application during analysis, which reduces the risk of isomerization of unsaturated FAs, and they offer the advantages of speed, resolution, high sensitivity, and specificity (Obert et al. 2007; Funazo et al. 1989). In HPLC, to improve the ultraviolet or fluorescence detectability of weakly chromophoric FAs, derivatization with sensitive chromophoric groups (naphthacyl esters, nitrobenzyl, and naphthaliminoethyl esters, or phenacyl, phenylazophenacyl, and methyl esters) has been used (Rioux et al. 1999; Obert et al. 2007; Funazo et al. 1989; Yasaka et al. 1990; Wood and Lee 1983; Vioque et al. 1985; Aveldano et al. 1983; Mansour 2005). The more frequently used methyl ester derivatization procedure enhanced the sensitivity enough to allow the detection of FAs. Due to the chemical characteristics of FAs, the majority of FA derivative separations by HPLC are reverse-phase (RP) systems. In RP-HPLC mode, both the retention and the selectivity increase as the alkyl chain of the bonded phase is lengthened (Wu et al. 2016; Mansour 2005; Christie et al. 2007). In addition to RP-HPLC, other modes of liquid chromatography such as argentation (Ag$^+$-HPLC) and ion-pair liquid chromatography (IP-HPLC) have also been widely applied for the analysis of specific FAs (Winkler and Steinhart 2001; Adlof 2004; Villegas et al. 2010; Delmonte et al. 2008; Tsuyama et al. 1992). Until now, the RP-HPLC in isocratic mode is still the most commonly used technique for HPLC of FAs. However, gradient elution which offers a superior dynamic range than that of isocratic elution has become popular for separating different groups of FAs. Although these methods are particularly suitable for the separation of

cis-/trans- isomers, simultaneous separation of FAs with different chain lengths and unsaturation in addition to cis-/trans-isomers is difficult (Lima and Abdalla 2002; Chen and Chuang 2002; Makahleh et al. 2010; Bravi et al. 2006; Rioux et al. 1999). In this regard, there is a great need for improving reverse-phase separation of FAs, which can also make possible the recovery of each FA's fraction for further analyses.

The present study deals with improving the separation, identification, and quantification of cis-/trans- isomers of long-chain unsaturated FAs in the RP-HPLC mode. The study involves the detailed optimization study of most effective method parameters such as %acetonitrile content in mobile phase, temperature, and flow rate by the evaluation of the response surface methodology (RSM) based on central composite design (CCD). It is well known that the CCD has several advantages over the classical "one-factor-at-a-time optimization experiments," since the factors involved in an experiment are being simultaneously altered. Therefore, by performing fewer experiments, the CCD provides more information along with individual as well as interactive effect of all the experimental parameters involved in the study (Walia et al. 2015; Lee et al. 2015; Ahmed et al. 2011; Trevisan and Arêas 2012). The optimized and validated conditions were also applied for the analysis of FAs in functional cold-pressed oils after the fatty acid methyl ester derivatization procedure.

Experimental

Chemicals, Standards, and Samples

HPLC-grade acetonitrile and methanol were purchased from VWR International (Poole, UK) and Sigma-Aldrich (St. Louis, USA). Deionized water (> 18 MΩ cm) was obtained from a Milli-Q system (Millipore, Brussels, Belgium). All other chemicals and reagents were of analytical grade and obtained from Sigma-Aldrich (St. Louis, USA) and Merck (Darmstadt, Germany). The certified fatty acid (FA) reference material, Supelco 37 Component FAME Mix, was obtained from Sigma-Aldrich (St. Louis, USA). A total of 14 cold-pressed oil samples [walnut oil (WO), black seed oil (BSO), pumpkin seed oil (PSO), poppy seed oil (PO), safflower oil (SFO), hemp oil (HO), wheat germ oil (WGO), linseed oil (LSO), pomegranate seed oil (PGSO), grape seed oil (GSO), coriander oil (CO), sesame oil (SSO), fig seed oil (FSO), and nettle seed oil (NSO)] were purchased from local drugstores in Konya, Turkey.

Derivatization of Fatty Acids

Stock solutions of fatty acid methyl ester standards were prepared in acetonitrile at a concentration of 0.2 μg μL^{-1} and stored at −20 °C before analyses. The injection volumes of standards and samples were changed from 5 to 45 μL in

order to obtain the appropriate concentrations. FAs of cold-pressed oils were converted to fatty acid methyl ester (FAME) derivatives before analysis, and their relative content was calculated as a percentage of the total FAs. FAMEs were prepared according to the Annex XA of EEC 2568/91 procedure by some modifications (EEC 2568/91 1991). Briefly, 0.01 g of the oil sample was weighed into a centrifuge tube and dissolved in 10 mL of acetonitrile. Then, 0.10 mL of 2 N potassium hydroxide solution prepared by methanol was added and the tube was shaken for 60 s. This solution was subjected to centrifugation for 5 min at 4000 rpm, and the upper layer of the sample was filtered through a 0.45-μm polytetrafluoroethylene membrane filter. The solutions were transferred to a HPLC vial to determine the fatty acid profiles of cold-pressed oils.

Instrumentation

The fatty acid composition analyses were performed on the Agilent 1200 Series HPLC system (Agilent Technologies Inc., USA) consisting of a G1311A model quaternary pump, a G1328B model standard auto-sampler, a G1316A model thermostatted column compartment, and a G4212B model photodiode array detector (DAD). Different lengths of flexible peek tubing and connection components were used to provide connections among the system parts. The system was controlled by Agilent Chemstation 2001 software, and data were recorded using a data processor.

The analyses were performed by using Develosil C30 (250 × 4.6 mm, 5 μm; Phenomenex Inc., USA) and Nova-Pak C18 (150 and 300 × 3.9 mm, 4 μm in series; Waters Inc., USA) stainless-steel columns. The mobile phases were acetonitrile/water (A) and acetonitrile (B) used through the following gradient: 0–25 min: acetonitrile/water and 25–110 min: acetonitrile, was optimized according to the central composite design (CCD) study (Mansour 2005). Also, the temperature of the column compartment and flow rate parameters were optimized as reported in "Response Surface Methodology Study Based on Central Composite Design." The optimum injection volume of cold-pressed oil samples was 25 μL, and injections were carried out at least three times. The derivatives were detected spectrophotometrically at 200 and 210 nm using a photodiode array detector. Detection of the FAs was accomplished by comparing retention times with that of approved commercial standards of FAME, and results were calculated as percentage of FAs.

System Validation

Based upon International Conference on Harmonization (ICH) principles of validation (Validation of analytical procedures 2005), the data was validated using optimized method

conditions. The most significant parameters, system suitability, precision, linearity, and accuracy, were assessed.

Response Surface Methodology Study Based on Central Composite Design

In response surface methodology (RSM), the most commonly used experimental design to assess a second-order polynomial estimate of response in a particular region is a CCD. The CCD can be used to optimize the chromatographic separation of long-chain fatty acid isomers and to assist the development of better understanding of interactions between several experimental factors affecting separation quality. In this study, important experimental parameters of the RP-HPLC/DAD method were optimized by the evaluation of CCD. The selection of these factors was made on the preliminary experimental studies and prior researches from literature as well as system limitations, such as pressure, temperature,... etc. The factors selected for optimization were flow rate (mL min^{-1}) (X_1), temperature (°C) (X_2), and acetonitrile content in mobile phase (%acetonitrile) (X_3). Each factor was studied at five levels (−1.68, −1, 0, +1, +1.68) and the range and levels of these variables are presented in Table 1.

A total of 23 experiments, 14 possible combinations of both independent factors and 9 central points, were performed. RSM calculations were performed using the experimental design matrixes generated by Excel database (Microsoft, 2010) and Design-Expert v9 (Stat-Ease Corporation, USA). The response surface plots were also originated using MATLAB R2007b (MathWorks, USA) software. The relationship between the responses and levels of each factor could be illustrated by expressing the second-order polynomial equations via the figure of three-dimensional (3D) surface plots.

Method Validation

The validation of the method was performed and calibration data including retention time, linearity with the correlation coefficient of the calibration curves, limits of detection (LOD) and quantification (LOQ), and precision as a relative standard deviation (RSD) were presented. The validation procedure was performed for both stationary phases, Develosil C30 and Nova-Pak C18 columns, by using optimized parameters. The validation experiments were performed in 5 days ($n = 5$), and recovery studies were performed at three different mass fraction levels. The calibration was carried out by injecting the set of FAME standards in triplicate, on each day ($n = 5$). Calibration curves were created by plotting the peak area versus the mass fraction ratios for detected fatty acids. Stock solutions of FAME standards were prepared in acetonitrile at a concentration of 0.2 μg μL^{-1}, and the injection volumes of standards were changed at five different target mass fraction levels from 5 to 45 μL. The values were selected

Table 1 Coded and actual levels of variables for CCD matrix

Factors (variables)	Symbol, X_i	Levels of the factors				
		−1.68	−1	0	+1	+1.68
Flow rate (mL min^{-1})	X_1	0.332	0.4	0.5	0.6	0.668
Column temperature (°C)	X_2	6.6	10	15	20	23.4
ACN content in mobile phase (%)	X_3	66.6	70	75	80	83.4

taking into account both the method sensitivity and different fatty acid contents for refined or cold-pressed oils. The linearity of each calibration curve was estimated by the residual plots and calculation of the correlation coefficients. To calculate the LOD and LOQ of the proposed methods, on each of the 5 days of the validation, FAME standards were spiked at a level related to the lowest point of the calibration curve. LOD and LOQ values were calculated as 3 and 10 times, and the standard deviation of the signal was declared in absorbance units.

Statistical Analysis

The software used for data acquisition was Agilent Chemstation 2001. The software MATLAB R2007b (MathWorks, USA), Design-Expert v9 (Stat-Ease Corporation, USA), Excel database (Microsoft, 2010), and OriginPro 8 (OriginLab, USA) were applied to design and analyze the data. Analysis of variance, ANOVA, was used to assess the statistical significance and validation of models via Design-Expert v 10 and Excel database. The relationships between the response values and coded level variables could be demonstrated by expressing the polynomial equations and 3D surface plots.

Results

Optimization by Response Surface Methodology (RSM) Based on Central Composite Design (CCD)

The optimization study by using RSM based on the CCD was employed for identifying the simple and interactive effects of experimental variables of RP-HPLC/DAD for separation of FAs. The proposed optimization methodology comprises the following five major steps: (i) performing the statistically designed experiments, (ii) estimating the coefficients in second-order polynomial mathematical models, (iii) predicting response values and comparing these values with experimental data, (iv) visualizing of the inter-relationships between factors via response surface plots, and (v) validating the proposed model statistically (Brereton 1997; Lundstedt et al. 1998).

In the present study, by using the "one-factor-at-a-time approach," the preliminary experiments were performed to achieve a more realistic CCD model (data not presented). Based on these experiments, three independent variables were

chosen for the CCD optimization study and the variables were set within the limit values given in Table 1. CCD includes the planer full factorial design (FFD) along with an additional central point in such a way that $2^f = N$ (f = number of factors/variables). In this way, CCD is composed of $2^f + 2f + 1$ experiments along with some additional central points ($n = 7$) to guess the experimental error. A total of 23 experiments were performed; response values (Rs, N, α, and k' values) are the mean value of three results, and relative standard deviation (RSD %) is lower than 0.5 (Tables 2 and 3).

Tables 2 and 3 present the factorial design matrix along with response values related to the tested variables on RP-HPLC/DAD of FAs for Develosil C30 and Nova-Pak C18 columns, respectively. The results obtained from the CCD were also fitted with a second-order polynomial expression model with linear, polynomial, and cross terms. This model can be described as Eq. (1):

$$y = \beta_0 + \beta_1 \cdot X_1 + \beta_2 \cdot X_2 + \beta_3 \cdot X_3 + \beta_{11} \cdot X_1{}^2 + \beta_{22}$$
$$\cdot X_2{}^2 + \beta_{33} \cdot X_3{}^2 + \beta_{12} \cdot X_1 \cdot X_2 + \beta_{13} \cdot X_1 \cdot X_3$$
$$+ \beta_{23} \cdot X_2 \cdot X_3 + \beta_{123} \cdot X_1 \cdot X_2 \cdot X_3 \qquad (1)$$

where y represents the response value; β_0 is a constant which shows where the line intersects the y-axis and allows the average impact of the factors; β_1, β_2, and β_3 are regression coefficients; and β_{12}, β_{13}, β_{23}, and β_{123} are the regression coefficients for the interaction of variables (Brereton 1997). Thus, this model has been utilized to find out the way in which the factors should be varied to optimize the RP-HPLC/DAD parameters for long-chain FA separation. In this direction, by using the response values (Rs, N, α, and k' values) and the coded values, an empirical relationship between the response and independent variables was achieved and the obtained coefficients were expressed by the second-order polynomial equations. To evaluate the outcome of CCD experiments, the Rs, N, α, and k' values of certain peaks (FAME C22:6 and C18:3) were used (Coleman et al. 2001).

Optimum Conditions for Reverse-Phase Develosil C30 HPLC Column

A number of reverse-phase HPLC methods have been reported for the separation of *cis-/trans-* isomers of long-chain

Table 2 CCD matrix and results with 5 levels/3 factors for optimization study of RP-HPLC/DAD method parameters by using a 45-cm Nova-Pak C18 column

Variables for the central composite face-centered design (CCD) matrix with 5 levels and 3 factors—Nova-Pak C18 RP-HPLC column

Exp. no.	X_1 mobile phase flow rate (mL min⁻¹)	X_2 column temperature (°C)	X_3 ACN content (%)	Response value, Rs		Response value, N		Response value, α		Response value, k'	
				Experimental	Predicted	Experimental	Predicted	Experimental	Predicted	Experimental	Predicted
1	−1 (0.4)	−1 (10)	−1 (70)	3.06	3.00	177,146.25	183,455.80	1.04	1.04	2.81	2.87
2	1 (0.6)	−1 (10)	−1 (70)	2.93	2.75	175,526.41	180,980.69	1.04	1.04	2.79	2.98
3	−1 (0.4)	1 (20)	−1 (70)	2.20	2.21	168,817.68	172,193.78	1.04	1.03	2.71	2.69
4	1 (0.6)	1 (20)	−1 (70)	1.46	1.37	169,252.57	171,773.39	1.04	1.02	3.56	3.67
5	−1 (0.4)	−1 (10)	1 (80)	2.65	2.70	130,808.66	132,764.76	1.03	1.04	2.92	2.89
6	1 (0.6)	−1 (10)	1 (80)	1.95	1.88	108,614.54	109,715.37	1.04	1.03	3.65	3.74
7	−1 (0.4)	1 (20)	1 (80)	1.90	2.01	107,473.50	106,496.16	1.03	1.04	2.78	2.66
8	1 (0.6)	1 (20)	1 (80)	1.26	1.26	84,752.48	82,919.86	1.03	1.02	3.46	3.47
9	0 (0.5)	0 (15)	0 (75)	1.97	1.91	148,187.62	144,937.39	1.03	1.03	3.26	3.25
10	−1.68 (0.332)	0 (15)	0 (75)	2.82	2.73	154,381.56	150,190.96	1.03	1.04	2.46	2.56
11	1.68 (0.668)	0 (15)	0 (75)	1.44	1.61	131,546.31	129,392.06	1.03	1.02	3.91	3.71
12	0 (0.5)	−1.68 (6.6)	0 (75)	2.72	2.85	172,378.39	165,713.76	1.03	1.04	3.37	3.22
13	0 (0.5)	1.68 (23.4)	0 (75)	1.44	1.39	134,509.94	134,829.72	1.03	1.02	3.17	3.22
14	0 (0.5)	0 (15)	−1.68 (66.6)	2.26	2.42	204,397.09	196,041.98	1.03	1.03	3.08	2.92
15	0 (0.5)	0 (15)	1.68 (83.4)	1.88	1.80	77,898.58	79,908.83	1.03	1.03	3.09	3.15
16	0 (0.5)	0 (15)	0 (75)	2.00	1.91	150,097.15	144,937.39	1.03	1.03	3.27	3.25
17	0 (0.5)	0 (15)	0 (75)	1.95	1.91	147,552.94	144,937.39	1.04	1.03	3.25	3.25
18	0 (0.5)	0 (15)	0 (75)	1.95	1.91	146,197.76	144,937.39	1.02	1.03	3.25	3.25
19	0 (0.5)	0 (15)	0 (75)	1.93	1.91	143,779.77	144,937.39	1.03	1.03	3.25	3.25
20	0 (0.5)	0 (15)	0 (75)	1.83	1.91	142,412.77	144,937.39	1.03	1.03	3.23	3.25
21	0 (0.5)	0 (15)	0 (75)	1.85	1.91	141,693.90	144,937.39	1.02	1.03	3.23	3.25
22	0 (0.5)	0 (15)	0 (75)	1.85	1.91	141,693.90	144,937.39	1.02	1.03	3.23	3.25
23	0 (0.5)	0 (15)	0 (75)	1.85	1.91	141,693.90	144,937.39	1.02	1.03	3.23	3.25

Values are reported as means of three replicate analyses ($n = 3$)

Table 3 CCD matrix and results with 5 levels/3 factors for optimization study of RP-HPLC/DAD method parameters by using a 25-cm Develosil C30 column

Variables for the central composite face-centered design (CCD) matrix with 5 levels and 3 factors—Develosil C30 RP-HPLC column

Exp. no.	X_1 mobile phase flow rate (mL min^{-1})	X_2 column temperature (°C)	X_3 ACN content (%)	Response value, Rs		Response value, N		Response value, α		Response value, k'	
				Experimental	Predicted	Experimental	Predicted	Experimental	Predicted	Experimental	Predicted
1	−1 (0.4)	−1 (10)	−1 (70)	2.15	2.14	120,747.85	145,445.99	1.03	1.03	2.94	3.05
2	1 (0.6)	−1 (10)	−1 (70)	2.09	1.83	122,059.77	117,467.44	1.03	1.03	2.93	3.21
3	−1 (0.4)	1 (20)	−1 (70)	1.48	1.51	149,586.22	146,535.87	1.02	1.02	2.87	2.79
4	1 (0.6)	1 (20)	−1 (70)	0.77	0.54	213,081.65	180,740.84	1.01	1.01	3.73	3.81
5	−1 (0.4)	−1 (10)	1 (80)	1.95	1.94	104,683.45	110,145.29	1.03	1.03	3.19	3.32
6	1 (0.6)	−1 (10)	1 (80)	2.06	1.79	121,959.00	98,130.38	1.03	1.03	2.93	3.22
7	−1 (0.4)	1 (20)	1 (80)	1.11	1.13	90,014.08	67,727.45	1.02	1.02	3.08	3.01
8	1 (0.6)	1 (20)	1 (80)	0.91	0.68	341,057.68	289,480.57	1.01	1.01	3.77	3.87
9	0 (0.5)	0 (15)	0 (75)	1.00	1.00	120,817.34	120,065.62	1.02	1.01	3.46	3.47
10	−1.68 (0.332)	0 (15)	0 (75)	2.12	1.97	120,529.31	104,706.59	1.03	1.03	2.94	2.99
11	1.68 (0.668)	0 (15)	0 (75)	0.71	1.18	141,495.25	195,411.74	1.01	1.02	4.15	3.81
12	0 (0.5)	−1.68 (6.6)	0 (75)	1.99	2.20	127,343.00	113,355.97	1.03	1.03	3.59	3.20
13	0 (0.5)	1.68 (23.4)	0 (75)	0.47	0.59	150,859.34	202,940.14	1.01	1.01	3.40	3.49
14	0 (0.5)	0 (15)	−1.68 (66.6)	1.24	1.39	129,879.98	126,026.51	1.02	1.02	3.17	3.03
15	0 (0.5)	0 (15)	1.68 (83.4)	1.01	1.18	73,702.57	115,649.81	1.02	1.02	3.42	3.26
16	0 (0.5)	0 (15)	0 (75)	1.00	1.00	120,817.34	120,065.62	1.01	1.01	3.46	3.47
17	0 (0.5)	0 (15)	0 (75)	1.00	1.00	120,817.34	120,065.62	1.02	1.01	3.46	3.47
18	0 (0.5)	0 (15)	0 (75)	1.00	1.00	120,817.34	120,065.62	1.02	1.01	3.46	3.47
19	0 (0.5)	0 (15)	0 (75)	1.00	1.00	120,817.34	120,065.62	1.02	1.01	3.46	3.47
20	0 (0.5)	0 (15)	0 (75)	1.00	1.00	120,817.34	120,065.62	1.02	1.01	3.46	3.47
21	0 (0.5)	0 (15)	0 (75)	1.00	1.00	120,817.34	120,065.62	1.02	1.01	3.46	3.47
22	0 (0.5)	0 (15)	0 (75)	1.00	1.00	120,817.34	120,065.62	1.02	1.01	3.46	3.47
23	0 (0.5)	0 (15)	0 (75)	1.00	1.00	120,817.34	120,065.62	1.02	1.01	3.46	3.47

Values are reported as means of three replicate analyses ($n = 3$)

unsaturated FAs. They are mostly based on C18 columns and various solvent systems, including acetonitrile (Juanéda 2002; Christie et al. 2007), acetonitrile/water (Mansour 2005), methanol/water (Bravi et al. 2006), acetonitrile/dichloromethane/propionitrile (Rezanka 2000a, b), and others. Most of the methods use acetonitrile in the mobile phase, which makes them potentially appropriate for the layout of the double bonds (DBs). Thus, we have improved the separation, identification, and quantification of *cis-/trans-* isomers of long-chain unsaturated FAs in RP-HPLC mode by using two kinds of column, Develosil C30 (25 cm × 0.46 cm, 5 μm) and Nova-Pak C18 (15 and 30 cm × 0.39 cm, 4 μm in series) stainless-steel columns. The detailed optimization study for most effective method parameters was performed, by the evaluation of RSM based on the CCD. The separations were optimized using a standard containing 37 unsaturated FAMEs with an even and odd number of carbons and up to 6 double bonds.

Four important chromatographic parameter Rs, N, α, and k' were selected as a response value in proposed models. By using this response and the coded values, an empirical relationship between the response and independent variables was attained. The obtained coefficients for each response value by using the Develosil C30 column were described by the following second-order polynomial Eqs. (2–5).

$$
\begin{aligned}
y = \mathrm{Rs}\ value = {}& 0.995293398-0.235034648 \\
& \cdot X_1-0.478877069 \cdot X_2-0.061695617 \\
& \cdot X_3 + 0.206385561 \cdot X_1{}^2 \\
& + 0.141172551 \cdot X_2{}^2 + 0.103350324 \\
& \cdot X_3{}^2-0.119916828 \cdot X_1 \cdot X_2 \\
& + 0.085243383 \cdot X_1 \cdot X_3 \\
& + 0.001373215 \cdot X_2 \cdot X_3 \\
& + 0.043530492 \cdot X_1 \cdot X_2 \cdot X_3 \quad (2)
\end{aligned}
$$

$$
\begin{aligned}
y = N\ value = {}& 120,065.6204 + 26,995.57957 \cdot X_1 \\
& + 26,661.95359 \cdot X_2-3088.305738 \cdot X_3 \\
& + 10,626.96531 \cdot X_1{}^2 + 13,492.92659 \\
& \cdot X_2{}^2 + 273.7174098 \cdot X_3{}^2 \\
& + 36,993.94385 \cdot X_1 \cdot X_2 \\
& + 25,438.97429 \cdot X_1 \cdot X_3 \\
& + 10,571.13331 \cdot X_2 \cdot X_3 \\
& + 21,448.06637 \cdot X_1 \cdot X_2 \cdot X_3 \quad (3)
\end{aligned}
$$

$$
\begin{aligned}
y = \alpha\ value = {}& 1.014991722-0.004860423 \\
& \cdot X_1-0.008358815 \cdot X_2-0.000132047 \\
& \cdot X_3 + 0.003149595 \cdot X_1{}^2 \\
& + 0.001805005 \cdot X_2{}^2 + 0.002216149 \\
& \cdot X_3{}^2-0.002930107 \cdot X_1 \cdot X_2 \\
& + 0.000206191 \cdot X_1 \cdot X_3 \\
& + 7.17856E{-}05 \cdot X_2 \cdot X_3-6.65288E{-}05 \\
& \cdot X_1 \cdot X_2 \cdot X_3 \quad (4)
\end{aligned}
$$

$$
\begin{aligned}
y = k'\ value = {}& 3.469368711 + 0.242571715 \cdot X_1 \\
& + 0.084514934 \cdot X_2 + 0.068655387 \\
& \cdot X_3-0.025466158 \cdot X_1{}^2-0.04464955 \\
& \cdot X_2{}^2-0.114823422 \cdot X_3{}^2 \\
& + 0.229502131 \cdot X_1 \cdot X_2-0.052153639 \\
& \cdot X_1 \cdot X_3-0.000577329 \cdot X_2 \cdot X_3 \\
& + 0.011520223 \cdot X_1 \cdot X_2 \cdot X_3 \quad (5)
\end{aligned}
$$

To compute the coded optimum points from the proposed model, the partial derivatives of this model were taken to zero, and by executing the matrix functions for each response value, the obtained optimum values were X_1 (flow rate) = 1.27, X_2 (temperature) = 2.24, and X_3 (%ACN content) = −0.24 for the Rs response value; X_1 = 1.31, X_2 = −3.30, and X_3 = 3.60 for the N response value; X_1 = 2.98, X_2 = 4.74, and X_3 = −0.19 for the α response value; and X_1 = −0.81, X_2 = −1.13, and X_3 = 0.48 for the k' response value. Afterwards, these coded values were converted to actual values which correspond to X_1 (flow rate) = 0.63 mL min^{-1}, X_2 (temperature) = 26.2 °C, and X_3 (%ACN content) = 73.8% for the Rs response value; X_1 = 0.63 mL min^{-1}, X_2 = 1.15 °C, and X_3 = 93.0% for the N response value; X_1 = 0.80 mL min^{-1}, X_2 = 38.7 °C, and X_3 = 74.1% for the α response value; and X_1 = 0.42 mL min^{-1}, X_2 = 9.4 °C, and X_3 = 77.4% for the k' response value (Table 4).

The impacts of the three different variables on response values for the Develosil C30 RP-HPLC column were visualized in 3D response surface plots (Fig. 1 and Supplementary Fig. 1), which show the interactive effects of two factors on chromatographic separation parameters. From the 3D response surface plots, the optimal values of the independent variables could be monitored, and the interaction between the pair of each independent variable can be simply understood. It can be revealed from Fig. 1 that the k' response value varies considerably with the variation of each variable in its range with non-linear relationship between response and

Table 4 Optimum coded and actual values of the RP-HPLC/DAD method for responses

Factors		Optimum coded and actual values of the RP-HPLC/DAD method for responses							
		Rs		N		α		k′	
		Coded	Actual	Coded	Actual	Coded	Actual	Coded	Actual
Nova-Pak C18 column	Flow rate (mL min^{-1}), X_1	3.20	0.82 mL min^{-1}	2.81	0.78 mL min^{-1}	2.09	0.71 mL min^{-1}	5.97	1.10 mL min^{-1}
	Temperature (°C), X_2	5.28	41.4 °C	−2.12	4.4 °C	2.73	28.7 °C	−2.29	3.6 °C
	ACN in mobile phase (%), X_3	−1.41	67.9%ACN	−2.06	64.7%ACN	−1.06	69.7%ACN	5.23	101.2%ACN
Develosil C30 column	Flow rate (mL min^{-1}), X_1	1.27	0.63 mL min^{-1}	1.31	0.63 mL min^{-1}	2.98	0.80 mL min^{-1}	−0.81	0.42 mL min^{-1}
	Temperature (°C), X_2	2.24	26.2 °C	−3.30	1.5 °C	4.74	38.7 °C	−1.13	9.4 °C
	ACN in mobile phase (%), X_3	−0.24	73.8%ACN	3.60	93.0%ACN	−0.19	74.1%ACN	0.48	77.4%ACN

RSM graphs for the optimization of RP-HPLC/DAD separations by Develosil C30 column

a %ACN & column temperature (response; k')

b flow rate & column temperature (response; k')

c flow rate & %ACN (response; k')

d Normal probability of internally studentized residuals (response; k')
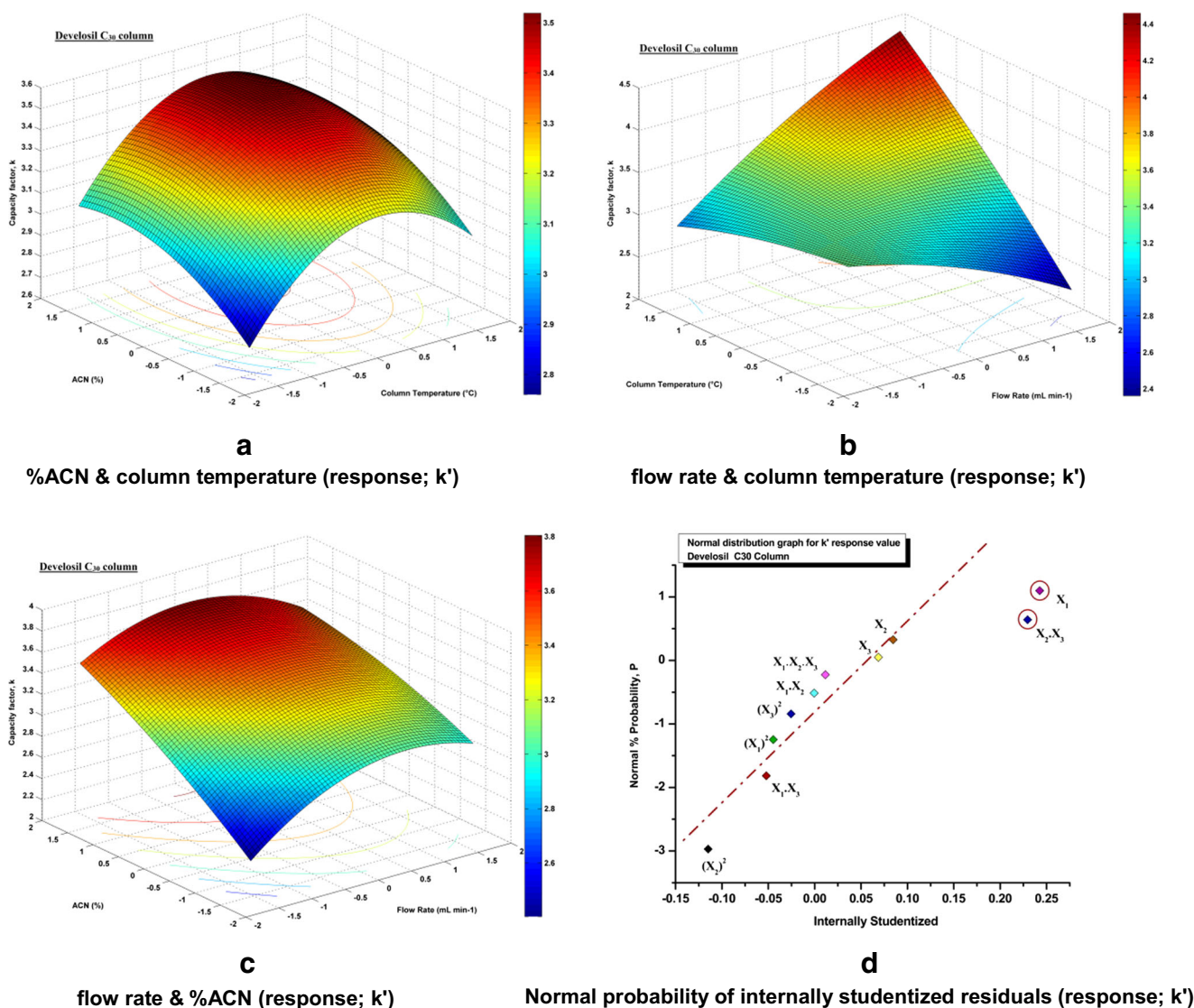
Fig. 1 RSM graphs for the optimization of RP-HPLC/DAD separations by Develosil C$_{30}$ column on $k′$ response value estimated from the CCD by plotting of (**a**) %ACN content versus temperature, (**b**) temperature versus flow rate, (**c**) flow rate versus %ACN content (**d**) normal probability of internally studentized residuals

variables as the surface plots illustrate the curves. Figure 1a illustrates the variation in response to the change of %acetonitrile content in mobile phase (66.6–83.4%) and column temperature (6.6–23.4 °C); it reveals a trend in which with the increasing %acetonitrile content and temperature the response value increases and reaches its maximum at %acetonitrile 77.4% (code +0.48) and temperature 9.4 °C (code −1.13) and again decreases with the increase in values of corresponding variables. These findings can be described by the fact that, at low acetonitrile content of the mobile phase, the migration rate of FAs on a column takes a very long time, and thus, there is a greater possibility for FA isomer separation, while at 77.4% acetonitrile, the separation of FAs reaches the desired condition; hence, any further increase in acetonitrile causes a decrease in separation efficiency. On the other hand, the shape of the horizontal oval seems to be on center (Fig. 1a) which reveals that the acetonitrile content in the mobile phase and temperature have an equal effect on the k' response value. Whereas, Fig. 1b presents the effect of column temperature and flow rate of the mobile phase on the k' response value which represents the increase in the k' response value with temperature and reaches the maximum point at temperature 23.4 °C (code +1.68) and decreases with a decrement in temperature, whereas with the increase in flow rate, the k' response value also increases and becomes maximum at 0.668 mL min^{-1} (code +1.68) and decreases with a decrement in temperature between variables. These results can be explained by the fact that the separation of FAs has an identical effect on the k' response value and the retention factor of FA isomers is considerably affected by both variables. Figure 1c illustrates the effect of %acetonitrile content in mobile phase and flow rate on the k' response values which represent the increase in response value with temperature and reaches the maximum point at %acetonitrile content 77.4% (code +0.48) and decreases with any further change in acetonitrile, whereas with the increase in flow rate, the response value also increases and becomes maximum at 0.42 mL min^{-1} (code −0.81) with no significant effect between mentioned variables.

The effects of experimental factors were also adopted to evaluate the adequacy of the preferred CCD model. To evaluate the effects of the flow rate of the mobile phase, temperature, and acetonitrile content in the mobile phase, normal probability plots were drawn and given in Fig. 1 and Supplementary Fig. 1.

The elution order of the FAMEs on the Develosil C30 column used in this study was not much different from that known for the shorter-chain C18 columns (Fig. 2) (Bravi et al. 2006; Juanéda 2002; Rezanka 2000a, b). As can be seen from Fig. 2b, the retention time increased with the chain length and decreased with the increasing number of double bonds.

The isomers varying in the DB geometry, such as C18:1n−9c/C18:1n−9t; C18:2n−6cc/C18:2n−6tt, separated from each other; the *cis*-isomers had lower retention times. The isomers differing in the positions of the DBs such as C18:3n−3/C18:3n−6; C20:3n−3/C20:3n−6 were also separated, but with lower resolution.

Optimum Conditions for Reverse-Phase Nova-Pak C18 HPLC Column

A CCD optimization study was also performed (Table 1) for the Nova-Pak C18 HPLC column, which is known to provide an excellent resolution for lipids (Kofroňová et al. 2009; Lísa and Holčapek 2008; Vrkoslav et al. 2010). When compared to the chromatographic performance with a C30 column, C18 systems were roughly equally efficient and provided symmetrical peaks (Fig. 2). However, the C30 column offered a substantially better resolution of the FAME peaks; the FAMEs eluted in 15 peaks within 65 min (Fig. 2). The alteration of the column temperature selectivity is another way to affect chromatographic separations; thus, we attempted to get better peak-to-peak resolution of FAME isomers using the Nova-Pak C18 column (Fig. 3). It is well known that the retention of compounds in chromatography columns varies with changed column temperatures, and the retention time of FA peaks is highly decreased with an increment in the column temperature. Thus, the excellent isomeric separation of FA isomers and an improvement for the Nova-Pak C18 column were observed at lower-column-temperature applications.

The separations were optimized using a mix of the unsaturated FAME standards, and the coded values, an empirical relationship between the response and independent variables was also attained by using the Rs, N, α, and k' response values. The obtained coefficients for each response values were described by the following second-order polynomial Eq. (6–9).

$$
\begin{aligned}
y = \text{Rs } value = {}& 1.905921078 - 0.331056873 \\
& \cdot X_1 - 0.435111891 \cdot X_2 - 0.1839091 \\
& \cdot X_3 + 0.093679881 \cdot X_1^2 \\
& + 0.076066281 \cdot X_2^2 + 0.072492411 \\
& \cdot X_3^2 - 0.066824019 \cdot X_1 \\
& \cdot X_2 - 0.059342459 \cdot X_1 \cdot X_3 \\
& + 0.109506802 \cdot X_2 \cdot X_3 \\
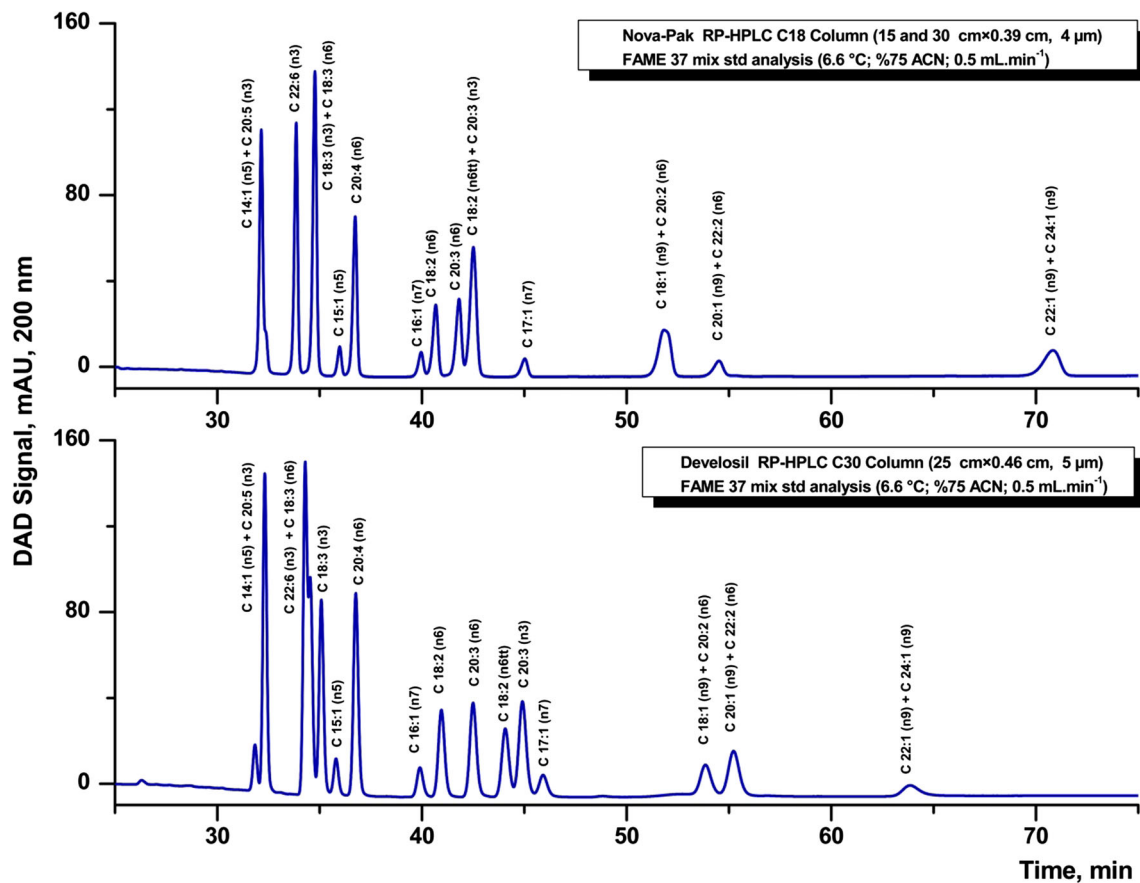& + 0.082784886 \cdot X_1 \cdot X_2 \cdot X_3 \quad (6)
\end{aligned}
$$

Fig. 2 Comparison of the Develosil C_{30} and Nova-Pak C_{18} column separations for the FAME-37 standard mixture

$y = N\ value = 144,937.3947 - 6190.14752$
$\cdot X_1 - 9191.679909 \cdot X_2 - 34,563.43978$
$\cdot X_3 - 1823.230921 \cdot X_1^2 + 1890.003777$
$\cdot X_2^2 - 2466.691104 \cdot X_3^2$
$+ 190.9785404 \cdot X_1 \cdot X_2 - 5466.274231$
$\cdot X_1 \cdot X_3 - 4074.348497 \cdot X_2$
$\cdot X_3 - 322.7036346 \cdot X_1 \cdot X_2 \cdot X_3$ (7)

$y = \alpha\ value = 1.026902511 - 0.005069786$
$\cdot X_1 - 0.005305839 \cdot X_2 + 0.001092383$
$\cdot X_3 + 0.001804188 \cdot X_1^2$
$+ 0.001805005 \cdot X_2^2 + 0.002121993$
$\cdot X_3^2 - 0.001221817 \cdot X_1$
$\cdot X_2 - 0.000799308 \cdot X_1 \cdot X_3$
$+ 0.001863543 \cdot X_2 \cdot X_3 + 0.00127256$
$\cdot X_1 \cdot X_2 \cdot X_3$ (8)

$y = k'\ value = 3.246366623 + 0.342644715$
$\cdot X_1 - 0.000174387 \cdot X_2 + 0.069340864$
$\cdot X_3 - 0.040455322 \cdot X_1^2 - 0.008828491$
$\cdot X_2^2 - 0.075097318 \cdot X_3^2$
$+ 0.102693343 \cdot X_1 \cdot X_2 + 0.071919692$
$\cdot X_1 \cdot X_3 - 0.124981842 \cdot X_2$
$\cdot X_3 - 0.114869713 \cdot X_1 \cdot X_2 \cdot X_3$ (9)

To calculate the coded optimum points from the proposed model, the partial derivatives of this model were taken to zero, and by executing the matrix functions for each response value, the obtained values for the Nova-Pak C18 column are given in Table 5. The effects of the three different variables on the response values for the Nova-Pak C18 RP-HPLC column were visualized in 3D response surface plots (Fig. 4 and Supplementary Fig. 2). To evaluate the effects of experimental factors, normal probability plots were also drawn and given in Fig. 4 and Supplementary Fig. 2.

Figure 4a presents the effect of %acetonitrile content and temperature on the k' response values which represent the increase in response value with temperature, and arrive
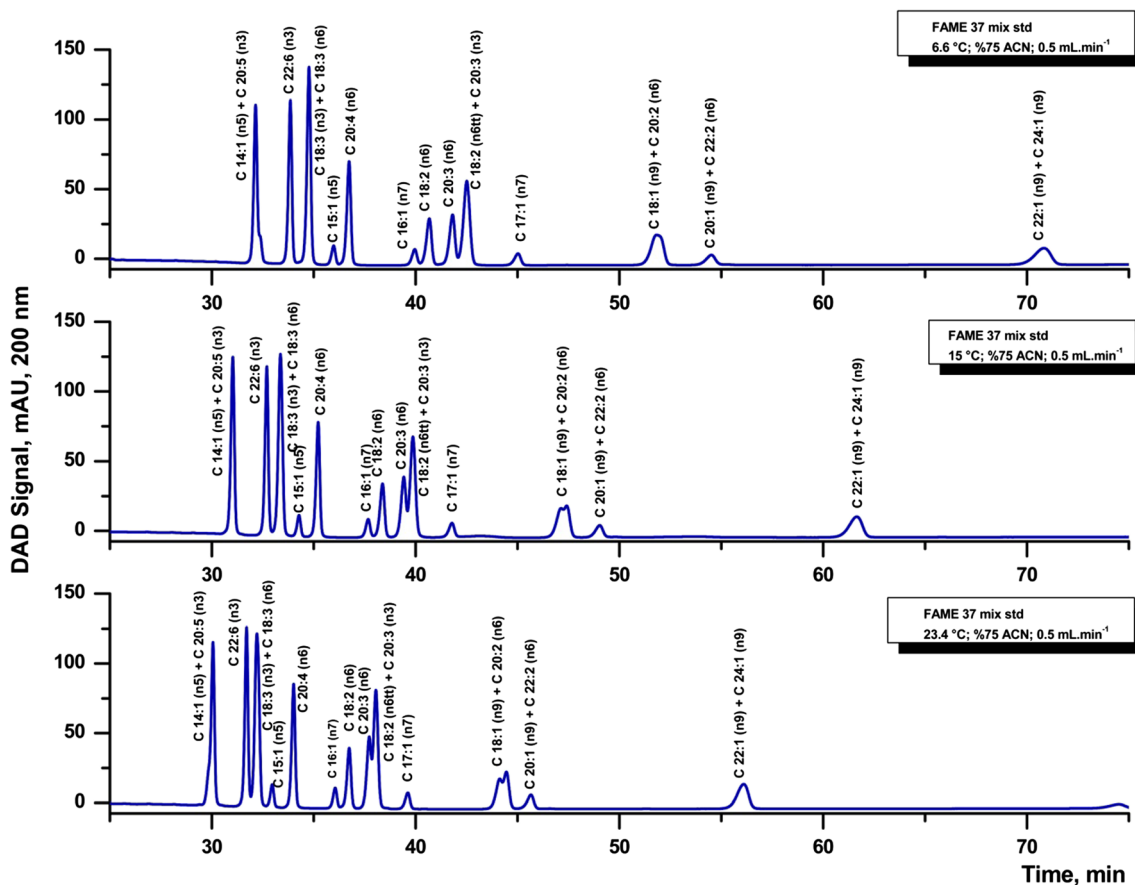
Fig. 3 RP-HPLC/DAD chromatograms of the FAME-37 standard mixture separated using Nova-Pak C_{18} column by using different column temperature applications

at the maximum point at %acetonitrile content 101.2% (code +5.23) and decreases with any further change in acetonitrile, whereas with the increase in temperature, the response value also increases and becomes maximum at 3.6 °C (code −2.29) without any significant effect between

revealed variables. These can be expressed by the fact that at low %acetonitrile content of the mobile phase, the elution of FAs takes a long time, and therefore, there is a greater possibility for separation. Besides, the shape of the horizontal oval seems to be on the cross corners of the graph which

Table 5 ANOVA test for validating and confirming the studied CCD model for the k' response value

Nova-Pak C18 column		ANOVA test for validating and confirming the experimental design model for k' response value				
		Degree of freedom	Sum of squares	Mean squares	$F_{experimental}$	P value
	Model	9	2.1396	0.2377	17.37*	$P < 0.0001$
	Residual	13	0.1779	0.0137		F value > F critical
	Lack of fit	5	0.1469	0.0294		
	Pure error	8	0.0310	0.0039		
	Total	22	2.3175			
						$P = 0.05$; $df_1/df_2 = 9/13 F_{critical} = 2.71*$
Develosil C30 column		ANOVA test for validating and confirming the experimental design model for k' response value				
		Degree of freedom	Sum of squares	Mean squares	$F_{experimental}$	P value
	Model	9	1.6577	0.1842	4.39*	$P < 0.05$
	Residual	13	0.5450	0.0419		F value > F critical
	Lack of fit	5	0.5140	0.1028		
	Pure error	8	0.0310	0.0039		
	Total	22	2.2028			
						$P = 0.05$; $df_1/df_2 = 9/13 F_{critical} = 2.71*$

⌐ Springer

RSM graphs for the optimization of RP-HPLC/DAD separations by Nova-Pak C18 column
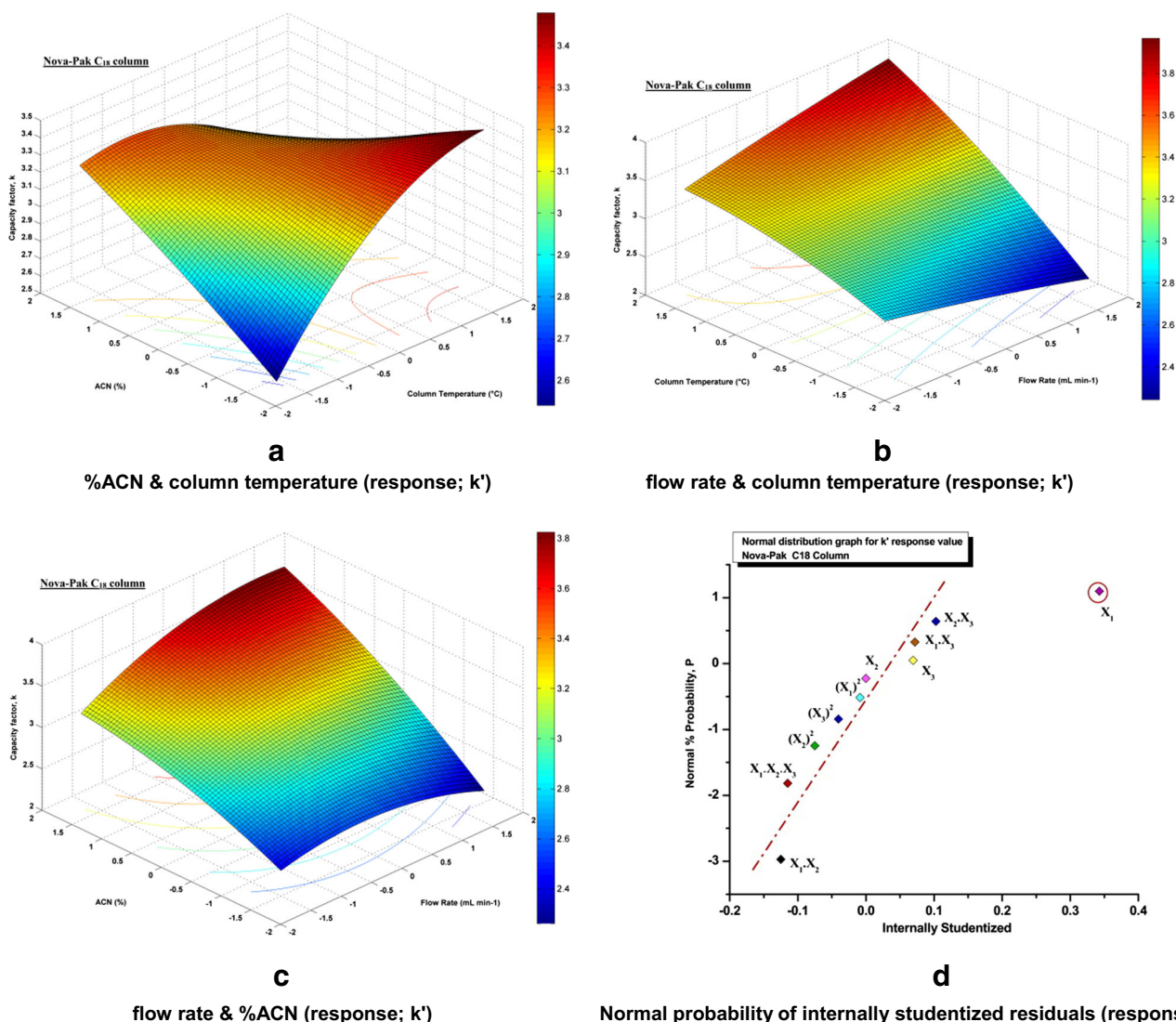

Fig. 4 RSM graphs for the optimization of RP-HPLC/DAD separations by Nova-Pak C_{18} column on k' response value estimated from the CCD by plotting of (**a**) %ACN content versus temperature, (**b**) temperature versus flow rate, (**c**) flow rate versus %ACN content (**d**) normal probability of internally studentized residuals

reveals that the variables have an equal effect on the response. Figure 4b illustrates the impact of temperature and flow rate variables on the k' response value, which represents the increase in the response value with temperature and reaches to a maximum point at temperature 27.7 °C (code +1.68) and decreases with a decrement in temperature, while with the increase in flow rate, the k' response value also increases and becomes maximum at 1.10 mL min^{-1} (code +5.97). These results can be explained by the fact that the separation of FAs has an identical effect on the k' response value and the retention factor of FA isomers is considerably affected by both variables. Also, Fig. 4c presents the effect of %acetonitrile content and flow rate on the k' response value which represents the increase

in response value with temperature and reaches the maximum point at %acetonitrile content 101.2% (code +5.23) and decreases with any further alteration in acetonitrile. With the increase in flow rate, the response value also increases and gets maximum at 1.10 mL min^{-1} (code +5.97) without any remarkable impact between the variables.

Discussion

Model and Method Validation

To check the adequacy and significance of proposed CCD models, ANOVA tests were performed for Develosil C30

and Nova-Pak C18 columns. The ANOVA table of the model for k' and other response values are presented in Table 5 and Supplementary Table 1, respectively. Analysis of variance partitions the total variation in the data into variation due to the factors and those due to the random factors. These components of variation were then used to calculate $F_{experimental}$ values. The calculated $F_{experimental}$ values are compared with the tabulated F distribution to designate at which probabilities (P value) the variables are significant. If $F_{experimental}$ is greater than the tabulated value of $F_{critical}$, this point is a good predictor of the experimental results (Asadollahzadeh et al. 2014). From the ANOVA of the empirical second-order polynomial model for the k' response value (Table 5), the $F_{experimental}$ value for the model is 17.37, indicating that the model is highly significant. This information reveals that the proposed CCD model for all response values is also significant and adequate with experimental conditions (Supplementary Table 1).

The accuracy of the CCD model, which compares the predicted and experimental values for k' response values, is presented in Fig. 5a. It can be revealed from these figures that the predicted values match the experimental values sensibly justifying the significance of the proposed models. The plots of residuals versus predicted responses are also given in Fig. 5b. As can be seen from these graphs, the divisions of residuals are casual without any trends. The results obtained show that the fitted models provide a high-quality approach to the relationship between the variables and k' response; in other words, they are adequate to evaluate the effect of selected variables by RSM.

To achieve separation of studied fatty acids and to maximize both sensitivity and precision of the methods, the validation procedure was performed. Fatty acid methyl esters were identified according to their t_R, and the statistical parameters calculated from least-square regression are presented in Table 6.
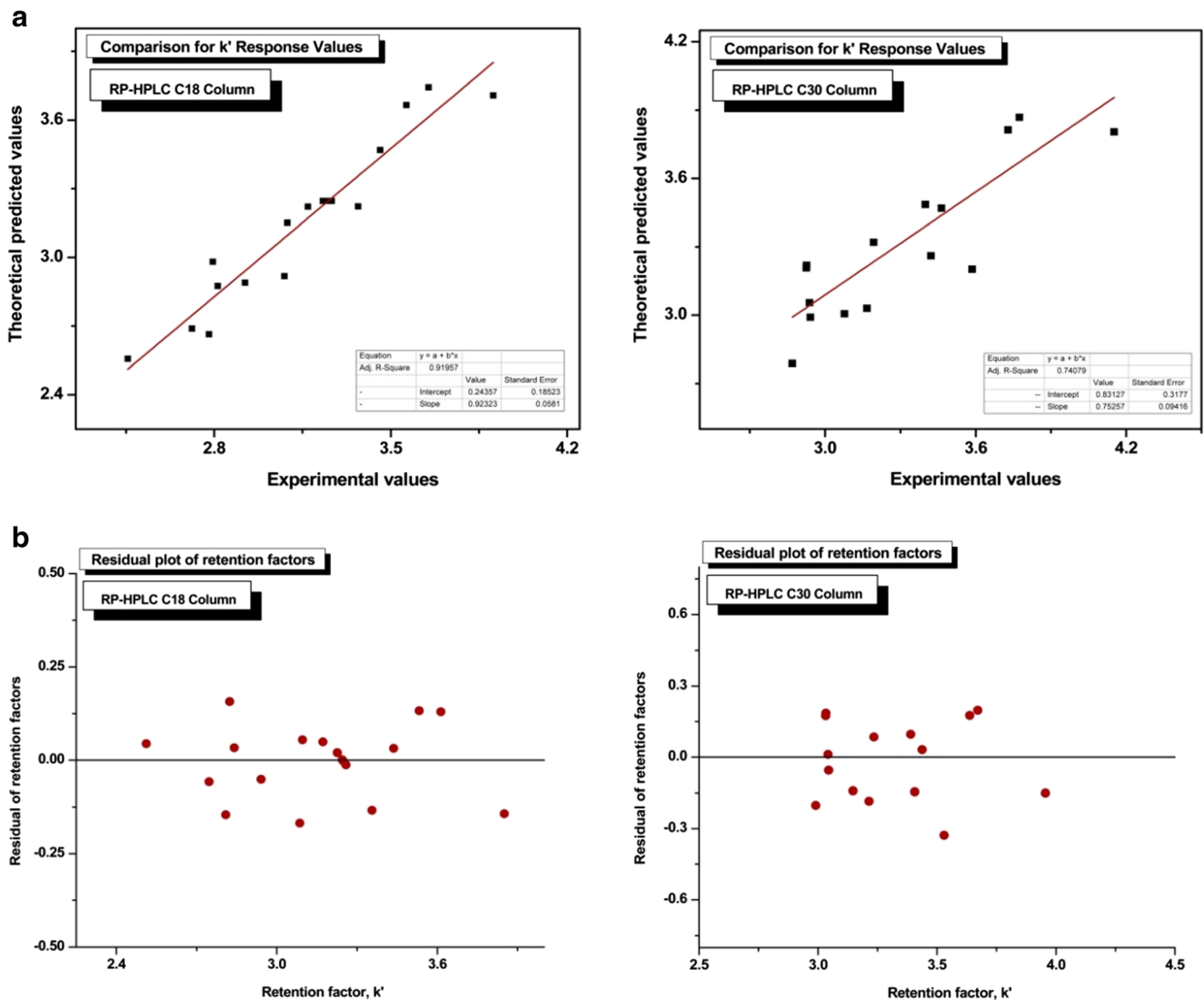

Fig. 5 Comparison of theoretical and experimental data (a) and residual plots (b) for optimization study by Develosil C_{30} and Nova-Pak C_{18} columns, for k' response value

Table 6 Working range and calibration equations of the FAMEs ($n = 5$) and performance characteristics of the proposed method

	FAMEs	t_R, min	Injection, µL	Concentration, µg	Calibration		%RSD	LOD	LOQ
					Equation	r			
Develosil C30 column	Linolenic acid (C18:3, n3)	35.079	5–45	1–9	$y = 15{,}740x + 91{,}524$	0.9943	5.1	2.0	4.3
	Ginkgolic acid (C15:1, n5)	35.798	5–45	1–9	$y = 14{,}488x + 12{,}541$	0.9883	4.3	2.3	4.4
	Arachidonic acid (C20:4, n6)	36.765	5–45	1–9	$y = 72{,}411x + 15{,}785$	0.9993	3.6	2.0	4.1
	Palmitoleic acid (C16:1, n7)	39.899	5–45	1–9	$y = 93{,}501x + 14{,}579$	0.9947	4.7	6.0	9.7
	Linoleic acid (C18:2, n6)	40.948	5–45	1–9	$y = 25{,}110x + 21{,}821$	0.9926	5.3	3.9	9.4
	Eicosatrienoic acid (C20:3, n6)	42.495	5–45	1–9	$y = 15{,}418x + 14{,}271$	0.9891	5.7	3.1	10.3
	Linoleic acid (C18:2, tt6)	44.071	5–45	1–9	$y = 85{,}311x + 12{,}245$	0.9986	6.5	5.3	17.7
	Eicosatrienoic acid (C20:3, n6)	44.907	5–45	1–9	$y = 94{,}641x + 17{,}871$	0.9958	2.9	4.1	13.7
	Heptadecenoic acid (C17:1, n7)	45.917	5–45	1–9	$y = 69{,}323x + 21{,}673$	0.9981	3.7	2.7	9.0
Nova-Pak C18 column	Docosahexaenoic acid (C22:6, n3)	33.854	5–45	1–9	$y = 86{,}251x + 84{,}367$	0.9948	6.1	3.8	12.7
	Ginkgolic acid (C15:1, n5)	35.979	5–45	1–9	$y = 83{,}496x + 24{,}756$	0.9892	5.3	3.3	11.0
	Arachidonic acid (C20:4, n6)	36.736	5–45	1–9	$y = 54{,}763x + 24{,}763$	0.9478	4.2	2.6	8.7
	Palmitoleic acid (C16:1, n7)	39.959	5–45	1–9	$y = 88{,}563x + 24{,}531$	0.9149	5.4	6.7	18.9
	Linoleic acid (C18:2, n6)	40.673	5–45	1–9	$y = 95{,}763x + 15{,}473$	0.9977	6.1	4.3	14.3
	Eicosatrienoic acid (C20:3, n6)	41.812	5–45	1–9	$y = 73{,}546x + 16{,}723$	0.9711	6.4	4.8	16.1
	Heptadecenoic acid (C17:1, n7)	45.025	5–45	1–9	$y = 99{,}476x + 21{,}463$	0.9843	4.0	3.2	10.7

r correlation coefficient, *LOD* limit of detection, *LOQ* limit of quantification, *RSD* relative standard deviation, *SD* standard deviation, t_R retention time

As can be seen from Table 6, the higher correlation co-efficients (*r*) were determined for all fatty acid methyl esters (0.9149–0.9993). The LODs and LOQs of each analyte were calculated by spiking three blank oil samples at the lowest level of the working range for each fatty acid. The LOD was theoretically estimated as 3 times the standard deviation, while the LOQ was estimated as 10 times the standard deviation obtained from analyses of independent samples at the lowest calibrated level. The repeatability and intermediate precision values in the study stated as RSD were calculated between 2.9 and 6.5%. Thus, the validation results present the good accuracy of the proposed method-ologies and so its suitability for the characterization of reference fatty acid materials.

Fatty Acid Profiles of Cold-Pressed Oils by RP-HPLC/DAD

The normalized percentages of the myristic (C14:0), palmitic (C16:0), *cis-/trans*-palmitoleic (C16:1), heptadecenoic (C17:0), *cis-10*-heptadecenoic (C17:1), stearic (C18:0), *cis-/trans*-oleic (18:1), *cis-/trans*-linoleic (18:2), *cis-/trans*-linolenic (C18:3), arachidic (C20:0), *cis-11*-eicosenoic (C20:1), *cis-11,14*-eicosadienoic (C20:2), heneicosanoic (C21:0), behenic (C22:0), tricosanoic (C23:0), and lignoceric (C24:0) acids in the commercial 14 cold-pressed oils are presented in Table 7.

The percentage distributions of each FA for the studied oils were clearly different, allowing oil kind identification and detection of adulteration by peak area comparisons. FA profiles are within the official ranges for cold-pressed oils specified in the Codex Alimentarius (Joint FAO/WHO Report 2001); therefore, the results obtained do not need any further comments. It is well known that FAs, which constitute a major portion of the saponifiable material in oils, are found in all fats and oils; their composition is characteristic of each cold-pressed oil, and it can be considered as a fingerprint (Van Ruth et al. 2010; Siang et al. 2010; Benitez-Sanchez et al. 2003). As can be seen in Table 7, fig seed (FSO) and nettle seed oils (NSO) were clearly distinguished by their FA profiles due to their far greater ∑SFA contents (35.14 and 40.9% values) than in the other oils. It is noteworthy that except these three kinds of oil, all cold-pressed oil varieties contain small amounts of SFAs (4.05–18.05%), whereas ∑PUFA range between 18.46 and 88.22%. The cold-pressed oils studied in this work also contain small amounts of ∑trans FAs (0.03–1.47%), and the content of ∑MUFA is relatively high (5.60–74.21%). The calculated values of RSD ranged between 0.001 and 0.21% indicating reasonable repeatability of the official methods for determination of FA composition.

Table 7 The results of fatty acid composition analysis for cold-pressed oils by using the optimized RP-HPLC/DAD method

Fatty acid composition analysis results of cold-pressed oils by using optimized RP-HPLC/DAD method, %

Fatty acids	Walnut oil	Sesame oil	Wheat germ oil	Poppy seed oil	Flaxseed oil	B. cumin seed oil	Pumpkin seed oil	Safflower oil	Hemp seed oil	Pomegranate seed oil	Grapeseed oil	Coriander oil	Fig seed oil	Nettle seed oil
C8:0	nd	nd	nd	nd	nd	nd	nd	nd	nd	nd	nd	nd	nd	nd
C10:0	nd	nd	nd	nd	nd	nd	nd	nd	nd	nd	nd	nd	nd	nd
C12:0	nd	nd	nd	nd	nd	nd	nd	nd	nd	nd	nd	nd	nd	nd
C14:0	0.02 ± 0.001	0.01 ± 0.001	nd	0.04 ± 0.001	nd	0.30 ± 0.001	0.09 ± 0.003	0.10 ± 0.001	0.05 ± 0.001	nd	0.03 ± 0.001	0.05 ± 0.002	0.15 ± 0.001	0.21 ± 0.001
C16:0	7.09 ± 0.02	7.66 ± 0.03	0.54 ± 0.01	9.17 ± 0.04	5.41 ± 0.03	12.25 ± 0.07	11.99 ± 0.06	6.21 ± 0.01	5.10 ± 0.02	0.72 ± 0.02	7.02 ± 0.02	3.90 ± 0.01	34.77 ± 0.20	35.17 ± 0.14
C16:1 t	0.01 ± 0.001	nd	nd	nd	nd	nd	nd	nd	nd	nd	nd	nd	nd	nd
C16:1	0.11 ± 0.002	0.01 ± 0.001	nd	0.12 ± 0.002	0.06 ± 0.001	0.21 ± 0.005	0.15 ± 0.004	0.10 ± 0.004	nd	nd	nd	0.42 ± 0.004	nd	0.70 ± 0.006
C17:0	0.08 ± 0.001	nd	2.44 ± 0.01	0.06 ± 0.001	0.04 ± 0.001	0.12 ± 0.001	0.11 ± 0.002	0.01 ± 0.001	0.04 ± 0.001	0.93 ± 0.001	0.02 ± 0.001	nd	nd	nd
C17:1	0.01 ± 0.001	nd	nd	0.04 ± 0.001	nd	nd	nd	0.06 ± 0.001	nd	nd	nd	nd	nd	nd
C18:0	2.80 ± 0.05	4.28 ± 0.04	1.07 ± 0.001	2.6 ± 0.03	3.75 ± 0.04	3.53 ± 0.02	5.61 ± 0.03	2.25 ± 0.01	1.57 ± 0.01	2.76 ± 0.01	2.51 ± 0.01	2.91 ± 0.02	0.19 ± 0.002	4.30 ± 0.02
C18:1 t	0.01 ± 0.001	0.01 ± 0.001	nd	nd	0.03 ± 0.001	0.04 ± 0.001	nd	0.02 ± 0.001	0.01 ± 0.001	nd	0.02 ± 0.001	0.06 ± 0.001	nd	0.01 ± 0.001
C18:1	17.62 ± 0.04	39.39 ± 0.15	7.38 ± 0.02	15.5 ± 0.04	23.10 ± 0.14	25.88 ± 0.21	27.60 ± 0.13	32.17 ± 0.09	10.98 ± 0.02	5.60 ± 0.04	13.87 ± 0.05	73.49 ± 0.05	5.99 ± 0.02	6.78 ± 0.04
C18:2 t	0.03 ± 0.001	0.02 ± 0.001	0.03 ± 0.001	0.03 ± 0.002	nd	nd	0.03 ± 0.001	0.07 ± 0.002	nd	nd	0.03 ± 0.001	nd	0.18 ± 0.001	0.02 ± 0.001
C18:2	59.73 ± 0.06	47.58 ± 0.04	17.39 ± 0.05	71.53 ± 0.03	16.77 ± 0.04	55.81 ± 0.08	53.26 ± 0.04	57.48 ± 0.02	59.77 ± 0.06	4.23 ± 0.08	75.52 ± 0.06	16.7 ± 0.03	58.62 ± 0.05	42.69 ± 0.04
C18:3 t	0.01 ± 0.001	nd	0.06 ± 0.001	0.13 ± 0.001	nd	nd	0.35 ± 0.001	0.21 ± 0.001	0.30 ± 0.001	1.47 ± 0.001	0.01 ± 0.001	nd	nd	0.01 ± 0.001
C20:0	0.07 ± 0.002	0.45 ± 0.004	nd	nd	0.36 ± 0.01	0.23 ± 0.01	nd	nd	nd	nd	nd	0.25 ± 0.01	nd	nd
C18:3	12.31 ± 0.05	0.57 ± 0.01	71.12 ± 0.05	0.55 ± 0.006	50.13 ± 0.09	0.82 ± 0.01	0.39 ± 0.01	0.55 ± 0.01	21.27 ± 0.02	83.99 ± 0.04	0.41 ± 0.004	1.76 ± 0.01	0.07 ± 0.005	6.78 ± 0.03
C20:1	nd	nd	nd	0.12 ± 0.001	nd	0.25 ± 0.002	0.15 ± 0.002	0.31 ± 0.002	0.78 ± 0.003	nd	0.52 ± 0.001	0.30 ± 0.002	nd	2.11 ± 0.002
C20:2	0.04 ± 0.001	nd	nd	0.03 ± 0.001	nd	nd	0.02 ± 0.001	0.02 ± 0.001	nd	nd	nd	nd	nd	nd
C21:0	nd	0.01 ± 0.001	nd	nd	nd	nd	nd	nd	nd	0.07 ± 0.002	0.02 ± 0.001	nd	nd	0.02 ± 0.001
C22:0	0.04 ± 0.002	0.01 ± 0.001	nd	0.08 ± 0.001	0.22 ± 0.003	0.42 ± 0.005	0.11 ± 0.001	0.31 ± 0.001	0.13 ± 0.001	nd	nd	0.15 ± 0.001	nd	1.20 ± 0.001
C23:0	nd	nd	nd	nd	nd	nd	0.06 ± 0.001	nd	nd	0.23 ± 0.001	nd	nd	nd	nd
C24:0	0.02 ± 0.001	nd	0.12 ± 0.001	nd	0.13 ± 0.002	0.14 ± 0.004	0.08 ± 0.001	0.13 ± 0.003	nd	nd	0.02 ± 0.001	nd	0.03 ± 0.001	nd
∑SFA	10.12	12.42	4.05	11.95	9.91	16.99	18.05	9.01	6.89	4.71	9.62	7.27	35.14	40.9
∑MUFA	17.74	39.4	7.38	15.78	23.16	26.34	27.9	32.64	11.76	5.60	14.39	74.21	5.99	9.59
∑PUFA	72.04	48.15	88.51	72.08	66.9	56.63	53.65	58.03	81.04	88.22	75.93	18.46	58.69	49.47
trans-FA	0.06	0.03	0.06	0.16	0.03	0.04	0.38	0.30	0.31	1.47	0.06	0.06	0.18	0.04

Means within a column are significantly different ($P < 0.01$). Values are reported as means ± SD of three replicate analyses ($n = 3$)

nd not detected

Conclusion

The reverse-phase HPLC separation of the *cis-/trans-* isomers of long-chain unsaturated fatty acids was optimized for Develosil C30 and Nova-Pak C18 columns, by the assessment of central composite design. The best separations were finally observed for the Develosil C30 column. The proposed second-order polynomial model, regression analysis, and 3D response surface plots pointed out 100 and 77.4% acetonitrile in mobile phases, 1.10 and 0.42 mL min^{-1} flow rates, and 3.6 and 9.4 °C temperatures as optimum for the effective Nova-Pak C18 and Develosil C30 column separations for the k' response value. Besides, $F_{\text{experimental}}$ values calculated from ANOVA were greater than the F_{critical} values at $P = 0.05$, suggesting that the proposed model is significant and adequate with experimental conditions. When compared to the chromatographic performance with the Develosil C30 column, the Nova-Pak C18 column was approximately equally efficient and provided symmetrical peaks; however, the Develosil C30 column offered a substantially better resolution of the FAME isomers. Regression analysis with R^2 values showed a good agreement between the experimental results and predicted values. Thus, by performing fewer experiments, CCD provides more information along with individual as well as interactive effect of all the experimental parameters involved in this study for a satisfactory separation of FAMEs.

Compliance with Ethical Requirements

Conflict of Interest Fatma Nur Arslan declares that she has no conflict of interest. Hacer Azak declares that she has no conflict of interest.

Ethical Approval All procedures performed in studies involving human participants were in accordance with the ethical standards of the institutional and/or national research committee and with the 1964 Helsinki declaration and its later amendments or comparable ethical standards.

Informed Consent Informed consent was obtained from all individual participants included in the study.

References

Adlof RO (2004) Separation of conjugated linoleic acid methyl esters by silver-ion high performance liquid chromatography in semi-preparative mode. J Chromatogr A 1033:369–371

Ahmed M, Akter MSTS, Eun J (2011) Optimization conditions for anthocyanin and phenolic content extraction form purple sweet potato using response surface methodology. Int J Food Sci Nutr 62(1):91–96

Asadollahzadeh M, Tavakoli H, Torab-Mostaedi M, Hosseini G, Hemmati A (2014) Response surface methodology based on central composite design as a chemometric tool for optimization of dispersive-solidification liquid–liquid micro-extraction for speciation of inorganic arsenic in environmental water samples. Talanta 123:25–31

Aveldano MI, Van Rollis M, Horrocks LA (1983) Separation and quantitation of free fatty acids and fatty acid methyl esters by reverse phase high pressure liquid chromatography. J Lipid Res 24:83–93

Bailey AL, Southon S (1998) Determination of total long-chain fatty acids in human plasma and lipoproteins, before and during copper-stimulated oxidation, by high-performance liquid chromatography. Anal Chem 70:415–419

Benitez-Sanchez PL, Leon-Camacho M, Aparicio R (2003) A comprehensive study of hazelnut oil composition with comparisons to other vegetable oils, particularly olive oil. Eur Food Res Technol 218:13–19

Bravi E, Perretti G, Montanari L (2006) Fatty acids by high-performance liquid chromatography and evaporative light-scattering detector. J Chromatogr A 1134:210–214

Brereton RG (1997) Multilevel multifactor designs for multivariate calibration. Analyst 122:1521–1529

Chen S, Chuang Y (2002) Analysis of fatty acids by column liquid chromatography. Anal Chim Acta 465:145–155

Christie WW, Dobson G, Adlof RO (2007) A practical guide to the isolation, analysis and identification of conjugated linoleic acid. Lipids 42:1073–1084

Coleman J, Wrzosek T, Roman R, Peterson J, McAllister P (2001) Setting system suitability criteria for delectability in high-performance liquid chromatography methods using signal-to-noise ratio statistical tolerance intervals. J Chromatogr A 917:23–27

Delmonte P, Hu Q, Kia ARF, Rader JI (2008) Preparation, chromatographic separation and relative retention times of cis/trans heptadecaenoic (17:1) fatty acids. J Chromatogr A 1214:30–36

European Union Commission EEC 2568/91 (1991) Characteristics of olive and olive pomace oils and their analytical methods. Off J Eur Communities L 248:1–82

Funazo K, Tanaka M, Yasaka Y, Takigawa H, Shono T (1989) New ultraviolet labelling agents for high-performance liquid chromatographic determination of monocarboxylic acids. J Chromatogr A 481:211–219

Gutnikov G (1995) Fatty acid profiles of lipid samples. J Chromatogr B Biomed Sci Appl 671:71–89

Joint FAO/WHO Food Standards Programme Codex Alimentarius Commission (2001) Report of the 17th Session of the Codex Alimentarius Committee on Fats and Oils. 19 – 23 February 2001, London, U.K

Juanéda P (2002) Utilisation of reversed-phase high-performance liquid chromatography as an alternative to silver-ion chromatography for the separation of cis- and trans-C18:1 fatty acid isomers. J Chromatogr A 954:285–289

Kofroňová E, Cvačka J, Vrkoslav V, Hanus R, Jiroš P, Kindl J, Hovorka O, Valterová I (2009) A comparison of HPLC/APCI-MS and MALDI-MS for characterising triacylglycerols in insects: species-specific composition of lipids in the fat bodies of bumblebee males. J Chromatogr B 877:3878–3884

Lacaze JCL, Stobo LA, Turrell EA, Quilliam MA (2007) Solid-phase extraction and liquid chromatography–mass spectrometry for the determination of free fatty acids in shellfish. J Chromatogr A 1145:51–57

Lee TZE, Krongchai C, Lu NA, Lu MI, Kittiwachana S, Sim SF (2015) Application of central composite design for optimization of the removal of humic substances using coconut copra. Int J Ind Chem 6: 185–191

Li C, Yao Y, Zhao G, Cheng W, Liu H, Liu C, Shi Z, Chen Y, Wang S (2011) Comparison and analysis of fatty acids, sterols, and tocopherols in eight vegetable oils. J Agric Food Chem 59:12493–12498

Lima ES, Abdalla DSP (2002) High-performance liquid chromatography of fatty acids in biological samples. Anal Chim Acta 465:81–91

Lísa M, Holčapek M (2008) Triacylglycerols profiling in plant oils important in food industry, dietetics and cosmetics using high-performance liquid chromatography–atmospheric pressure chemical ionization mass spectrometry. J Chromatogr A 1199:115–130

Lundstedt T, Seifert E, Abramo L, Thelin B, Nyström Å, Pettersen J, Bergman R (1998) Experimental design and optimization. Chemometr Intell Lab 42:3–40

Makahleh A, Saad B, Siang GH, Saleh MI, Osman H, Salleh B (2010) Determination of underivatized long chain fatty acids using RP-HPLC with capacitively coupled contactless conductivity detection. Talanta 81:20–24

Mansour MP (2005) Reversed-phase high-performance liquid chromatography purification of methyl esters of C_{16}–C_{28} polyunsaturated fatty acids in microalgae, including octacosaoctaenoic acid [28:8(n-3)]. J Chromatogr A 1097:54–58

Molnár-Perl I (2000) Role of chromatography in the analysis of sugars, carboxylic acids and amino acids in food. J Chromatogr A 891:1–32

Obert JC, Hughes D, Sorenson WR, McCann M, Ridley WP (2007) A quantitative method for the determination of cyclopropenoid fatty acids in cottonseed, cottonseed meal, and cottonseed oil by high-performance liquid chromatography. J Agric Food Chem 55:2062–2067

Rezanka T (2000a) Analysis of polyunsaturated fatty acids using high performance liquid chromatography–atmospheric pressure chemical ionization mass spectrometry. J High Resolut Chromatogr 23:338–342

Rezanka T (2000b) Analysis of very long chain polyunsaturated fatty acids using high-performance liquid chromatography–atmospheric pressure chemical ionization mass spectrometry. Biochem Syst Ecol 28:847–856

Rioux V, Catheline D, Bouriel M, Legrand P (1999) High performance liquid chromatography of fatty acids as naphthacyl derivatives. Analusis 27:186–193

Ruiz-Rodriguez A, Reglero G, Ibanez E (2010) Recent trends in the advanced analysis of bioactive fatty acids. J Pharm Biomed Anal 51:305–326

Siang GH, Makahleh A, Saad B, Lim BP (2010) Hollow fiber liquid-phase microextraction coupled with gas chromatography-flame ionization detection for the profiling of fatty acids in vegetable oils. J Chromatogr A 1217:8073–8078

Trevisan AJB, Arêas JAG (2012) Development of corn and flaxseed snacks with high-fibre content using response surface methodology (RSM). Int J Food Sci Nutr 63(3):362–367

Tsuyama Y, Uchida T, Goto T (1992) Analysis of underivatized C12–C18 fatty acids by reversed-phase ion-pair high-performance liquid chromatography with conductivty detection. J Chromatogr A 596:181–184

Validation of analytical procedures: text and methodology (2005) Complementary Guideline on Methodology

Van Ruth SM, Villegas B, Akkermans W, Rozijn M, van der Kamp H, Koot A (2010) Prediction of the identity of fats and oils by their fatty acid, triacylglycerol and volatile compositions using PLS-DA. Food Chem 118:948–955

Villegas C, Zhao Y, Curtis J (2010) Two methods for the separation of monounsaturated octadecenoic acid isomers. J Chromatogr A 1217:775–784

Vioque E, Maza MP, Millan F (1985) High-performance liquid chromatography of fatty acids as their p-phenylazophenacyl esters. J Chromatogr A 331:187–192

Vrkoslav V, Urbanová K, Cvačka J (2010) Analysis of wax ester molecular species by high performance liquid chromatography/atmospheric pressure chemical ionisation mass spectrometry. J Chromatogr A 1217:4184–4194

Walia A, Mehta P, Guleria S, Shirkot CK (2015) Improvement for enhanced xylanase production by Cellulosimicrobium cellulans CKMX1 using central composite design of response surface methodology. 3 Biotech 5:1053–1066

Wang XY, Wang HL, Liu YJ, You JM, Suo YR (2009) Extraction of pollen lipids by SFE-CO2 and determination of free fatty acids by HPLC. Eur J Lipid Sci Technol 111:155–163

Winkler K, Steinhart H (2001) Identification of conjugated isomers of linolenic acid and arachidonic acid in cheese. J Sep Sci 24:663–668

Wood R, Lee T (1983) High-performance liquid chromatography of fatty acids: quantitative analysis of saturated, monoenoic, polyenoic and geometrical isomers. J Chromatogr A 254:237–246

Wu Z, Zhang Q, Li N, Pu Y, Wang B, Zhang T (2016) Comparison of critical methods developed for fatty acid analysis: a review. J Sep Sci 40:1–11

Yasaka Y, Tanaka M, Shono T, Tetsumi T, Katakawa J (1990) 2-(2,3-Naphthalimino)ethyl trifluoromethanesulphonate as a highly reactive ultraviolet and fluorescent labelling agent for the liquid chromatographic determination of carboxylic acids. J Chromatogr A 508:133–140